Free Radical Research, April 2009; 43(4): 329–339

informa
healthcare

Effect of lipophilicity of Mn (III) *ortho N*-alkylpyridyl- and di*ortho* *N*, *N*′-diethylimidazolylporphyrins in two *in-vitro* models of oxygen and glucose deprivation-induced neuronal death

LISA WISE-FABEROWSKI[1], DAVID S. WARNER[1,2], IVAN SPASOJEVIC[3], & INES BATINIC-HABERLE[4]

[1]*Department of Anesthesiology,* [2]*Department of Neurobiology,* [3]*Department of Medicine, and* [4]*Department of Radiation Oncology, Duke University Medical Center, Durham, NC 27710, USA*

(Received 24 October 2008; revised 5 January 2009)

Abstract

In vivo investigations have confirmed the beneficial effects of hydrophilic, cationic Mn(III) porphyrin-based catalytic antioxidants in different models of oxidative stress. Using a cell culture model of rat mixed neuronal/glial cells, this study investigated the effect of MnTnOct-2-PyP^{5+} on oxygen and glucose deprivation (OGD)-induced cell death as compared to the effects of widely studied hydrophilic analogues MnTE-2-PyP^{5+} and MnTDE-2-ImP^{5+} and a standard compound, dizocilpine (MK-801). It was hypothesized that the octylpyridylporphyrin, MnTnOct-2-PyP^{5+}, a lipophilic but equally potent antioxidant as the other two porphyrins, would be more efficacious in reducing OGD-induced cell death due to its higher bioavailability. Cell death was evaluated at 24 h using lactate dehydrogenase (LDH) release and propidium iodide staining. At concentrations from 3–100 μM, all three porphyrins reduced cell death as compared to cultures exposed to OGD alone, the effects depending upon the concentrations and type of treatment. To assess the effect of lipophilicity the additional experiments were performed using submicromolar concentrations of MnTnOct-2-PyP^{5+} in an organotypic hippocampal slice model of OGD with propidium iodide and Sytox staining. When compared to oxygen and glucose deprivation alone, concentrations of MnTnOct-2-PyP^{5+} as low as 0.01 μM significantly ($p < 0.001$; power 1.0) reduced neuronal cells similar to control. This is the first *in vitro* study on the mammalian cells which indicates that MnTnOct-2-PyP^{5+} is up to 3000-fold more efficacious than equally potent hydrophilic analogues, due entirely to its increased bioavailability. Such remarkable increase in efficacy parallels 5.7-orders of magnitude increase in lipophilicity of MnTnOct-2-PyP^{5+} (log $P = -0.77$) when compared to MnTE-2-PyP^{5+} (log $P_{OW} = -6.43$), P_{OW} being partition coefficient between n-octanol and water.

Keywords: *MnTE-2-PyP^{5+} (AEOL10113), MnTnOct-2-PyP^{5+}, MnTDE-2-ImP^{5+} (AEOL10150), neuronal/glial cell culture, organotypic hippocampal slices (OHS), oxygen and glucose deprivation (OGD)*

Abbreviations: *MnTE-2-PyP^{5+}, Mn(III) meso-tetrakis(N-ethylpyridinium-2-yl)porphyrin (AEOL10113); MnTDE-2-ImP^{5+}, Mn(III) meso-tetrakis(N,N′-diethylimidazolium-2-yl)porphyrin (AEOL10150); MnTnOct-2-PyP^{5+}, Mn(III) meso-tetrakis(N-n-octylpyridinium-2-yl)porphyrin; MnTnHex-2-PyP^{5+}, Mn(III) meso-tetrakis (N-n-hexylpyridinium-2-yl)porphyrin; LDH, lactate dehydrogenase; SOD, superoxide dismutase; OGD, oxygen glucose deprivation; OHS, organic hippocampal slice*

Introduction

Oxidative stress is a key intracellular pathological condition that mediates neuronal death in the presence of oxygen and glucose deprivation (OGD) [1]. Recent pharmacological advances have allowed for the design of different superoxide dismutase (SOD) mimics such as Mn salen derivatives [2], Mn cyclic polyamines [3], nitroxide [4], MitoQ series of compounds [5,6] and

Correspondence: Lisa Wise-Faberowski, MD, University of Colorado at Denver Health Sciences Center, Department of Anesthesiology, 13123 East 16th Avenue, Aurora, CO 80045, Box 090, USA. Tel: 720-777-6224. Fax: (720) 777-7122. Email: lisa.faberowski@uchsc.edu; Ines Batinić-Haberle, Ph.D., Duke University Medical Center, Department of Radiation Oncology-Cancer Biology, P.O. Box 3455, Durham, NC 27710, Tel: 919-684-2101. Fax: 919-684-8718. Email: ibatinic@duke.edu.

ISSN 1071-5762 print/ISSN 1029-2470 online
DOI: 10.1080/10715760902736283

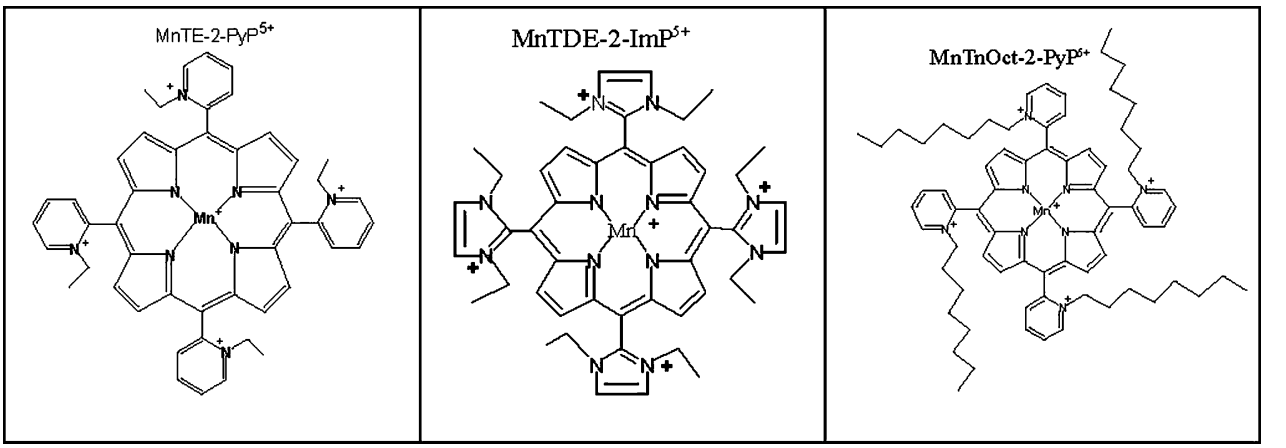

Figure 1. Mn porphyrins studied. Schematic drawings of cationic Mn(III) *ortho N*-alkylpyridyl- and di*ortho N, N′*-diethylimidazolylporphyrin-based catalytic antioxidants MnTE-2-PyP^{5+} (AEOL10113) and MnTDE-2-ImP^{5+} (AEOL 10150) in addition to more lipophilic but equally potent antioxidant, the octyl porphyrin, MnTnOct-2-PyP^{5+}.

Mn porphyrins (Figure 1) [7–10]. Most of them scavenge peroxynitrite also, though with different efficacy, Mn porphyrins being the most efficacious log $k_{red} \geq 7.5$ [7–12]. We have developed the most potent Mn porphyrins based on structure-activity relationships [7–12]. Those are Mn (III) *ortho* isomeric positively charged *N*-alkylpyridyl- or *N, N′*-dialkylimidazolylporphyrins (MnTalkyl-2-PyP^{5+}, MnTDalkyl-2-ImP^{5+}). They bear electron-deficient Mn centre that affords thermodynamic facilitation of the O_2^- dismutation. Their efficacy to remove superoxide parallels the efficacy to reduce peroxynitrite [11,12]. Further, they bear positive charges close to the Mn site that is needed for the electrostatic facilitation for the approach of negatively charged O_2^- and $ONOO^-$ [8]. MnTE-2-PyP, MnTDE-2-ImP^{5+} (Figure 1) and MnTnHex-2-PyP^{5+} offer remarkable protection in diseases that have oxidative stress in common such as cancer, diabetes, radiation injury, Alzheimer's [13–17]. They are also effective in central nervous system injuries; MnTE-2-PyP^{5+} and MnTDE-2-ImP^{5+} [18–20] have proven beneficial in middle cerebral artery occlusion models when given as late as 6h after the insult [21].

We have recently reported that if catalytic potency in scavenging superoxide and peroxynitrite is maintained, but lipophilicity increased, the efficacy *in vivo* increases tremendously (Table I) [9,13,22–24]. We increased lipophilicity up to 9-fold by increasing the length of the *N*-alkylpyridyl chains from 1 to 8 carbon atoms while maintaining identical antioxidant capacity (Table I) [9]. We initially measured lipophilicity by thin-layer chromatographic R_f value. R_f is the ratio of the compound path over solvent path on slica gel using solvent KNO_3saturated H_2O:H_2O: acetonitrile = 1:1:8. Using R_f values, the hexyl analogue, MnTnHex-2-PyP^{5+} is 4.3-fold more lipophilic than MnTE-2-PyP^{5+}. Such difference in R_f values lead to a 120-fold gain in efficacy in vivo; MnTnHex-2-PyP^{5+} is efficacious in several models of oxidative stress (*E. coli*, rat kidney ischemia/reperfusion, cerebral palsy, rat radioprotection, mice reversal of chronic morphine tolerance) at a lower dose (0.05–0.1 mg/kg) when compared to other synthetic antioxidants [9,13,22–24]. MnTnOct-2-PyP^{5+} (Figure 1) is ~ 6-fold more lipophilic than MnTE-2-PyP^{5+} based on thin-layer chromatographic R_f values (see Discussion) (Table I). Except in SOD-deficient *Escherichia coli* model [23], it has not been used in any other bacterial or mammalian model.

The enhanced bioavailability of MnTnOct-2-PyP^{5+} should promote improved neuronal survival as compared to hydrophilic compounds with fewer carbon atoms in the alkylpyridyl or dialkylimidazolyl chains [9,22–24]. We tested this hypothesis initially in mixed neuronal/glial cortical cell cultures exposed to OGD. Based on the findings in the preliminary investigation, we expanded our hypothesis using lower submicromolar concentrations (down to 0.01 μM) of MnTnOct-2-PyP^{5+} in an organotypic hippocampal slice (OHS) model of OGD. Unlike neuronal/glial cell cultures, OHS offers a model of intact neural circuits and avoid some of the variables inherent in *in vivo* investigations.

Methods

All animal procedures were approved by the Duke University (Durham, NC) Animal Care and Use Committees.

Experiment 1: Comparison of Mn (III) porphyrins to metal-free porphyrins in mixed neuronal-glial cell cultures

The experiment was performed to study MnTnOct-2-PyP^{5+} at doses previously used in similar studies with MnTE-2-PyP^{5+}; evaluate the effect of Mn site; and compare all three compounds at similar doses. This investigation was used as a foundation to determine the appropriate measure of cell death

Table I. The properties of Mn porphyrins: the ability to catalyse dismutation of $O_2^{\cdot-}$ (k_{cat}) and reduce $ONOO^-$ (k_{red}), the redox ability, i.e. the metal-centred redox potential ($E_{1/2}$) and the lipophilicity as given by (1) R_f values which represents the ratio of the compound and solvent path on TLC silica plates (solvent system, KNO_3sat H_2O:H_2O:acetonitrile = 1:1:8) and (2) by P_{ow}-values which describes the partition of the Mn porphyrin between n-octanol and water.

Compound	Log k_{cat} ($O_2^{\cdot-}$)	log k_{red} ($ONOO^-$)	$E_{1/2}$, mV vs NHE	R_f	log P_{OW}[a]
MnTE-2-PyP^{5+}[b]	7.76	7.53	+228	0.13	−6.25
MnTDE-2-ImP^{5+}[c]	7.83	7.00	+346	0.17	−6.08[d]
MnTnHex-2-PyP^{5+}	7.48	7.11	+314	0.57	−2.29
MnTnOct-2-PyP^{5+}[b]	7.71	7.15	+367	0.80	−0.77

[a][37]; [b][9] for k_{cat} ($O_2^{\cdot-}$) and 12 for k_{red}($ONOO^-$); [c][10] and Ferrer-Sueta and Batinic-Haberle (unpublished) for k_{red}($ONOO^-$) of MnTDE-2-ImP^{5+}; [d]predicted based on the comparison of R_f values for this compound and MnTE-2-PyP^{5+}.

when using the compounds in an OGD model of neuronal cell death. MK-801 [18,25] was used as a negative control.

Preparation of mixed neuronal-glial cell cultures. Mixed neuronal/glial cultures were prepared from foetal Sprague-Daley (Harlan Sprague Daley, Inc. Indianapolis, IN) rat brains at 18 days of gestation as previously described [18,25]. Brains were harvested from 10–15 pups and dissected to separate cortex from meninges and subcortical structures using anatomical landmarks. Cortices were pooled and minced into 2 mm^3 pieces in a buffered salt solution (BSS; Hanks Balanced Salt Solution (Life Technologies, Gaithersburg, MD) supplemented with 20 mM HEPES buffer (pH 7.4, containing 0.25% trypsin (Life Technologies)). The tissue was incubated for 20 min at 37°C in a 5% CO_2/95% room air atmosphere, then washed twice with ice-cold, glutamine-free minimum essential medium (MEM; Life Technologies) containing 15 mM glucose, 5% foetal bovine serum (Gibco Diagnostics, Inc., Madison, WI), 5% horse serum (GIBCO) and 1% DNase-I (Sigma Chemical Co., St. Louis, MO). Tissue pieces were dissociated by trituration through a fire-polished 9" Pasteur pipette. The resultant suspension was centrifuged at 50 g for 10 min, the supernatant discarded and the pellet resuspended in growth medium (MEM supplemented with 15 mM glucose, 5% foetal bovine serum and 5% horse serum). The dissociated cells were plated to achieve a confluent monolayer (4×10^5 cells per well for neuronal/glial cultures) on poly-D-lysine coated, 24-well culture plates (Falcon 3047; Becton Dickinson Co., Lincoln Park, NJ). Cultures were maintained undisturbed at 37°C in a humidified 5% CO_2/balance room air atmosphere for 10–14 days prior to use. Previous studies performed under identical culture conditions demonstrated cell types in 10 day old cultures to be 54 ± 4% neurons and 46 ± 7% glia as determined by immunohistochemical staining for cell-specific cytoskeletal filaments (neurofilament-160 for neurons and glial fibrillary acidic protein for astrocytes) [18–21,25–29].

Preparation of Mn (III) porphyrins and their related metal-free ligands. All compounds studied were synthesized as previously reported in detail [7,9,10,30]. Particular attention was paid to the purification of Mn porphyrins bearing longer alkyl chains. MnTnOct-2-PyP^{5+} was purified using ultrafilter 500-cut-off to eliminate excess of free Mn [30].

Effect of Mn porphyrins as compared to metal-free ligands. Based on previous studies, including our neuronal cell culture model work [25,27,29], 5 and 25 μM Mn porphyrins and their respective metal-free ligands were tested on the toxicity for 2.5 h as measured by LDH release in the absence of OGD. We aimed to compare the possible inherent toxicity of the metal-free compounds in our model in case some Mn is released from metal complexes during redox cycling. From our previous investigation in mixed neuronal-glial cell cultures, 100 μM of MnTDE-2-ImP^{5+} was toxic and 10 μm was most beneficial [18,25].

Oxygen and glucose deprivation. The original glucose containing media was removed from all treatment groups and replaced with a glucose-free BSS (7.65 g NaCl, 0.724 g Na_3PO_4 and 0.21 g K_3PO_4, pH 7.4). All media changes were followed by a wash with BSS. No serum was included in the glucose-free BSS. In the OGD phase, the media was washed with BSS and changed to hypoxic, glucose-free BSS. The glucose free/hypoxic BSS was prepared by passing the BSS through a microbubbler apparatus containing the hypoxic (94% N_2/6% CO_2, pH 7.37 ± 0.4) gas mixture. The 94% N_2/6% CO_2 gas mixture was used to maintain the previous incubating conditions without oxygen and with minimal change in pH. The hypoxic, glucose-free BSS was then applied in a thin layer (enough to cover the cells) to the cell culture dishes. Dishes exposed to hypoxia were then placed in a small, 3-litre, airtight experimental hypoxia chamber (Billups-Rothenberg; San Diego, CA) with inflow and outflow connectors. The experiments were conducted in a constant 37°C environment by placing the chambers in a water-jacketed incubator. The gaseous environment was controlled by the delivery of all gas via a heater humidifier (Fisher-Paykel; Laguna Hills, CA) servo-controlled to 37°C via the inflow adapter of the chamber. Delivered and

end-tidal concentrations of oxygen were monitored using a gas analyser (Datex Instruments Corporation, Tewksbury, MA) and maintained at $< 0.2\%$ [27].

As performed previously [18], cultures were exposed to conditions of oxygen and glucose deprivation for 2 h. The 3, 10, 30 and 100 μM concentrations for all three compounds were used for the first experiment in mixed neuronal cultures. Two experimental conditions were examined: (1) pre-treatment (30 min) prior to OGD and (2) pre-treatment (30 min) and continued treatment (2 h). All compounds were diluted in glucose-free BSS to provide the desired concentrations and immediately used for experimentation.

The exposure was terminated by removing the BSS, adding the original media for 24 h and then analysing for cell death as described below. Control cells were incubated in BSS in a normoxic incubator for the same time period as the experimental group.

Lactate dehydrogenase (LDH) release. Cellular injury was assessed 24 h after OGD by measuring the amount of LDH released by damaged cells into overlying medium. In brief, a 200-μl sample of culture medium was added to a polystyrene cuvette containing 10 mM lactate and 5 μmol of NAD^+ (β-nicotinamide adenine dinucleotide; Sigma, St. Louis, MO) in 2.75 ml of 50 mM glycine buffer pH 9.2 at 24°C. LDH activity was determined from the initial rate of reduction of NAD^+ as calculated using a linear least square curve fit of the temporal changes in fluorescence signal from the cuvette (340 nm excitation, 450 nm emission) and expressed in units of enzymatic activity (nmol of lactate converted to pyruvate per min). Analysis was performed on a fluorescence spectrophotometer (Perkin Elmer Model LS50B; Bodenseewerk GmbH, Uberlinger, Germany) [25].

Propidium iodide assay. The possible overlap of the absorbance of Mn porphyrin and LDH could have compromised our results. Thus, we used non-spectrophotometric analysis, propidium iodide fluorescence imaging as a measure of cell death. Propidium iodide is a highly fluorescent dye that penetrates damaged plasma membranes and binds to DNA [25]. Cells were exposed to a final concentration of 40 μg/ml of propidium iodide dissolved in BSS for 10 min. All staining procedures were done at room temperature. The cultures were then viewed under an inverted fluorescent microscope at 20× magnification with the observer blinded to treatment condition. Three fields were chosen in each separate well (10 wells for each experimental condition) for cell count determination per experiment. Dead cells were defined as those visibly stained by propidium iodide, which signals membrane disruption [25].

Experiment 2: Comparison of submicromolar MnTnOct-2-PyP^{5+} in an organotypic hippocampal slice model

Organotypic hippocampal slice (OHS) preparation. All studies were approved by the University of Colorado Health Sciences Center (Aurora, CO) Institutional Animal Care and Use Committee. OHS cultures were prepared according to the methods described by Stoppini et al. [28,29] with some modification. PND 9-11 Sprague Dawley rat pups (Zivic Laboratories, Pittsburgh, PA) were anaesthetized using an intraperitoneal injection of ketamine (10 mg/kg) and diazepam (0.2 mg/kg). The pups were decapitated and the hippocampi were removed and placed in 4°C Gey's Balanced Solution (Sigma-Aldrich, St. Louis, MO) with 100 μM adenosine. Using a MX-TS brain slicer (Siskiyou Design Instruments, Grants Pass, OR), the hippocampi were cut transversely (400 μm thickness) and transferred to 30-mm diameter membrane inserts (Millicell-CM, Millipore, Bedford, MA). Approximately 3–5 slices were placed within each well of a 6-well culture tray with media for 7 days before study. The culture media consisted of 50% Minimal Essential Media (Invitrogen, Carlsbad, CA), 25% Earle's Balanced Salt Solution (Invitrogen, Carlsbad, CA) and 25% Hyclone Heat Inactivated Horse Serum (Perbio, Cell Culture Division, South Logan, UT) with 6.5 mg/ml glucose and 5 mM KCl. The media was exchanged after the 2nd day in culture and 3–4 days later. OHS were cultivated in a humidified atmosphere at 37°C and 5% CO_2. No antibiotics or antimitotics were used.

Dose response. A dose response curve was determined using 0.01, 0.03, 0.1, 0.3, 1, 3 and 10 μM of MnTnOct-2-PyP^{5+}. MnTnOct-2-PyP^{5+} was diluted in glucose-free BSS to provide the desired concentrations and immediately used for experimentation.

Oxygen glucose deprivation. OHS with inserts were removed from the culture wells containing media and rinsed in BSS. One millilitre of hypoxic, glucose-free BSS was then placed in each well of the OHS culture dishes and the OHS with inserts were returned to their respective wells. Dishes exposed to hypoxia were then placed in a small, 3-l, airtight experimental hypoxia chamber (Billups-Rothenberg; San Diego, CA) with inflow and outflow connectors for 45 min.

Propidium iodide assay. Twenty-four hours after exposure to OGD and before imaging, the OHS media was replaced with media containing 2.3 μM of propidium iodide (Molecular Probes, OR) for 1 h.

The OHS were then viewed under an inverted fluorescent microscope at 20× magnification, using an Leica inverted microscope (2.5×) (Wetzlar, Germany) and fluorescent digital images were taken using a CoolSnap digital camera (Image Processing

Solutions, North Reading, MA), excitation wavelength 520 nm and emission 640 nm.

Both light and fluorescent microscopic images were made simultaneously for each slice and stored for later analysis. Three hippocampal regions were analysed: CA1, CA3 and dentate gyrus. Manual outlines of CA1, CA2, CA3 and dentate gyrus, on the images obtained by light microscopy, were superimposed on the fluorescent images using MCID software (Imaging Research, Inc. St. Catherines, Ontario, Canada). The mean optical density (fluorescence intensity) was then measured for each hippocampal region. Slices with intense fluorescence in hippocampal CA2 were excluded from analysis. These represented non-viable slices, which constituted ~5–10% of the OHS population. Analysis of the images was performed by an investigator blinded to group assignment and after completion of each experiment for consistency in measurement.

Sytox staining. Sytox (Molecular Probes, Eugene, OR) is a high affinity nucleic acid stain specific for cells with compromised plasma membranes and does not penetrate live cells [29,31,32]. Twenty-four hours after exposure to OGD and/or Mn-porphyrin, the media was exchanged with media containing 5 μM Sytox and was left unchanged for the remainder of the experiment. Three slices were imaged using a Leica inverted microscope (2.5×) (Wetzlar, Germany) and fluorescent digital images were taken using a CoolSnap digital camera (Image Processing Solutions, North Reading, MA), excitation wavelength 490 nm and emission 590 nm. The parameters for imaging were standardized for all slices. These images were compared to the bright field image of each individual slice. Hippocampal regions CA1, CA3 and dentate gyrus were outlined on the bright-field image. These outlines were transposed to the corresponding fluorescent image of the individual slice and the mean optical density (fluorescent intensity) was measured.

Statistical analysis. Data were compared by one-way analysis of variance. When indicated by a significant *F*-ratio and power, post-hoc testing was performed by use of Scheffe's test. Values are reported as mean ± SD. A *p*-value <0.05 was considered significant. Statistical analysis was performed using StatView 5.0 (SAS; Cary, NC).

Results

Experiment 1: Comparison of Mn (III) porphyrins to metal-free porphyrins in mixed neuronal-glial cell cultures

Dose response and LDH analysis. Concentrations of 5 μM and 25 μM of MnTDE-2-ImP^{5+} and MnTnOct-2-PyP^{5+} were analysed in mixed neuronal/glial cell cultures in the absence of OGD. The analysis demonstrated an elevation in cell death as compared to control cultures for all conditions (Table II). Furthermore, Mn complexes demonstrated more cell death than metal-free porphyrin compounds without Mn. Mn complexes might have stronger micellar character and are thus more toxic than the more hydrophobic [9] metal-free porphyrins. In both cases the toxicity of 5 μM and 25 μM concentrations was similar with all porphyrins and their metal-free ligands.

Table II. Dose response for 5 μM and 25 μM MnTDE-2-ImP^{5+} and MnTnOct-2-PyP^{5+} and their parent, metal-free porphyrins H_2TDE-2-ImP^{4+} and H_2TnOct-2-PyP^{4+} as measured by lactate dehydrogenase assay (LDH). Mixed neuronal/glial cell cultures were exposed to 5 μM and 25 μM of porphyrins for 2.5 h and LDH was determined 24 h later.

Condition	LDH (nmol of lactate converted to pyruvate per min), $M \pm$SD
Control	1.27±0.132
25 μM H_2TDE-2-ImP^{4+}	1.968±0.164
5 μM H_2TDE-2-ImP^{4+}	1.936±0.104
25 μM MnTDE-2-ImP^{5+}	2.784±0.472*
5 μM MnTDE-2-ImP^{5+}	2.912±0.541*
25 μM MnTnOct-2-PyP^{5+}	2.696±0.138
5 μM MnTnOct-2-PyP^{5+}	3.118±0.260
25 μM H_2TnOct-2-PyP^{4+}	2.512±0.359
5 μM H_2TnOct-2-PyP^{4+}	2.64±0.248

*$p<0.05$ as compared to non-Mn containing parent compound.

Two arms of the first experiment were used to determine neuronal/glial cell death using LDH analysis. These experiments are the following: (1) 30 min pre-treatment with the Mn porphyrins prior to OGD (Figure 2A) and (2) 30 min pre-treatment with continuation of the treatment during the 2 h of oxygen and glucose deprivation (Figure 2B). In both experiments, the conditions provided by 2 h of oxygen and glucose deprivation were statistically different than control and 10 μm MK801 ($p < 0.001$; $P=1.0$). Six wells were used for all conditions in both experiments.

Despite the toxicity of Mn porphyrins at 5 and 25 μM levels in the absence of OGD, the protection against OGD was observed in both arms of experiment 1 (Figure 2A and B). The toxicity is presumably outbalanced by the protectiveness, with concentrations as high as 100 μM Mn porphyrins. In the first arm of experiment 1, all compounds at all concentrations statistically decreased oxygen and glucose deprivation-induced LDH release ($p<0.001$), except for 3 μM MnTDE-2-ImP^{5+} and 10 and 30 μM of the MnTnOct-2-PyP^{5+}. The best protection was exerted with 100 μM MnTE-2-PyP^{5+}.

In the second arm of experiment 1, when compared to control conditions, 30 μM MnTE-2-PyP^{5+} ($p=0.296$) exerted best protection; it demonstrated similar LDH release as control. When compared to cells stressed by oxygen and glucose deprivation, statistical significance was achieved with 3, 10 and

30 μM MnTnOct-2-PyP^{5+}, MnTE-2-PyP^{5+} and MnTDE-2-ImP^{5+} (Figure 2B).

Propidium iodide staining. As demonstrated by our previous investigation, 10 μM MnTDE-2-ImP^{5+} was most efficacious in reducing neuronal cell death as compared to OGD ($p < 0.001$; $P = 1.0$). The reduction in cell death was similar to that provided by control conditions (Figure 3).

Experiment 2: Comparison of submicromolar concentrations of MnTnOct-2-PyP^{5+} in an organotypic hippocampal slice model

Six cell culture wells, ~18–24 slices, were used for each experimental condition (Figure 4). When compared to control, the number of dead neurons in the OGD group was statistically different ($p < 0.001$; $P = 1.0$). Compared to OGD alone, all concentrations of MnTnOct-2-PyP^{5+} afforded significant protection against neuronal death ($p < 0.001$). All concentrations provided levels of neuronal death similar to control except for 10 μM due to the prevailing toxic effects; 10 μM was statistically different ($p < 0.001$) than all other concentrations. At concentrations ≥ 0.01 μM full protection was observed. MnTE-2-PyP^{5+} and MnTDE-2-ImP^{5+}, though, exert best efficacy in OGD model in the range of 10–100 μM concentrations (Figures 2 and 3). In comparison, the efficacy of MnTnOct-2-PyP^{5+} appeared to be up to 3000-fold higher (Figure 4).

Sytox. Similar to propidium iodide staining, ~18–24 slices were used for each experimental condition. All concentrations of MnTnOct-2-PyP^{5} were able to significantly reduce neuronal death ($p < 0.001$; 10 μM (0.032); $P = 1.0$). OGD-induced neuronal death was different than control ($p < 0.001$) (Figure 5). The

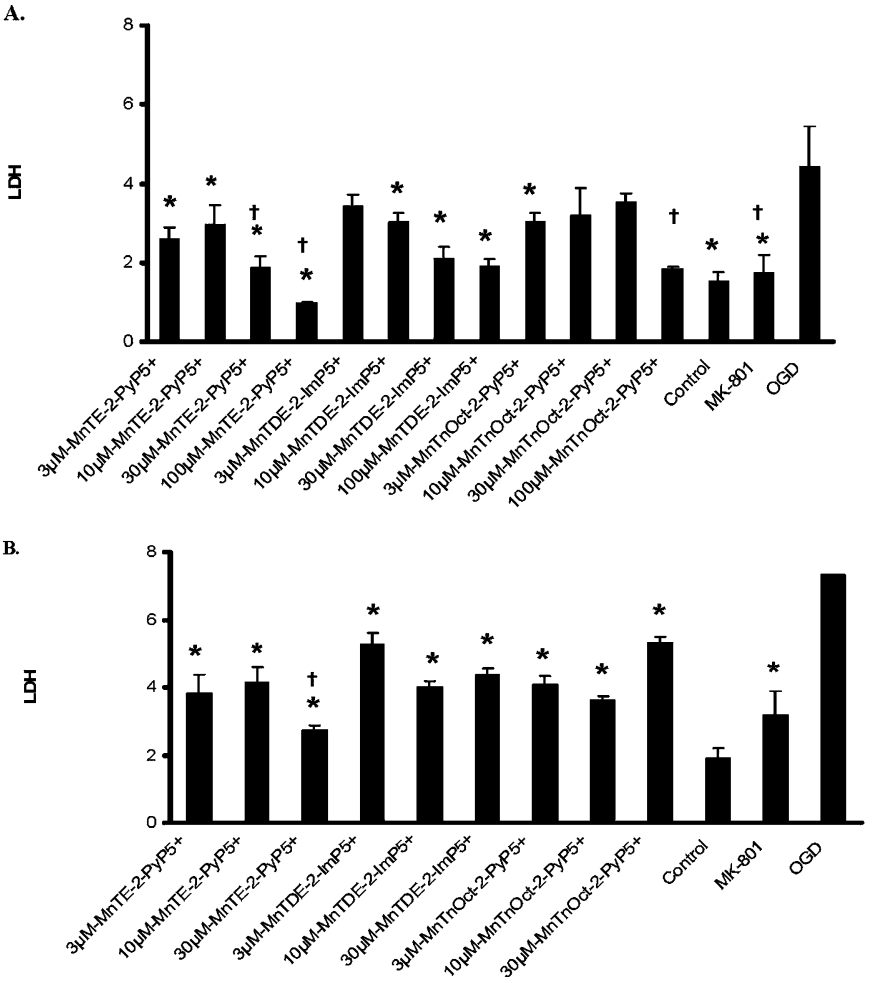

Figure 2. LDH (nmol of lactate converted to pyruvate per min) dose response curve: 30 min pre-treatment (A) prior to exposure to oxygen and glucose deprivation (OGD) and (B) with continued exposure during 2 h of oxygen and glucose deprivation (OGD). A dose response curve was determined at 24 h after (A) oxygen and glucose deprivation and (B) exposure to OGD, using previously *in vivo*/*in vitro* dosing (3, 10, 30 and 100 μM) of MnTE-2-PyP^{5+} and MnTDE-2-ImP^{5+}. The same doses were used for the MnTnOct-2-PyP^{5+} compound. These conditions were compared to (A) control and OGD and (B) control, OGD and 10 μM MK801. *Statistical difference ($p < 0.005$) from OGD; † statistically equal ($p > 0.999$) to control.

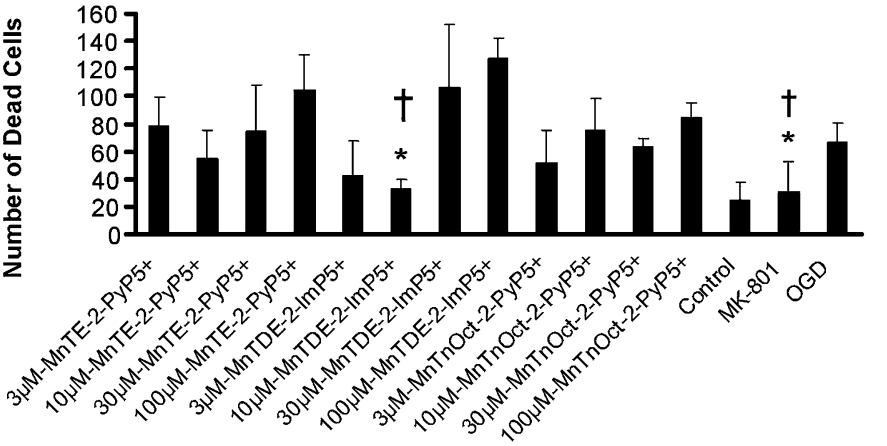

Figure 3. Cell death/propidium iodide assay in mixed neuronal/glial cell cultures: 30 min pre-treatment prior to exposure to oxygen and glucose deprivation with continued exposure during 2 h of oxygen and glucose deprivation. The number of dead cells was counted in three fields in each well and expressed as number of dead cells ± SD. Ten wells were examined for each experimental condition. *Statistical difference ($p < 0.005$) from oxygen and glucose deprivation (OGD); †statistically equal ($p > 0.999$) to control.

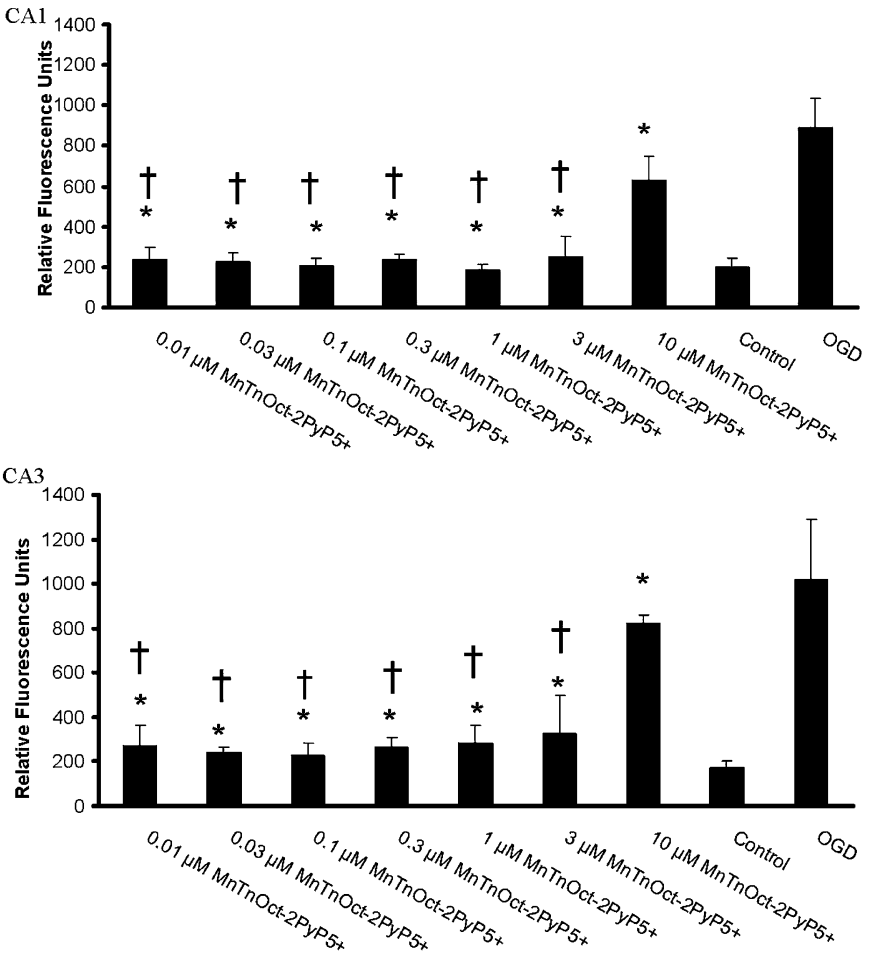

Figure 4. Cell death/propidium iodide staining of organotypic hippocampal slices (OHS): 30 min pre-treatment prior to exposure to oxygen and glucose deprivation with continued exposure during 45 min of oxygen and glucose deprivation—effects of submicromolar concentrations of MnTnOct-2-PyP^{5+}; 18–24 slices were examined for each condition. Relative fluorescence units ± SD are reported for each condition ($p < 0.05$). Areas CA1 (A) and CA3 (B) were evaluated. Regardless of region examined the data represents a statistical reduction in cell death with all concentrations of MnTnOct-2-PyP^{5+} as compared to OGD. All concentrations, except for 10 μM MnTnOct-2-PyP^{5+}, reduced neuronal cell death similar to control. There was no statistical significance amongst the six other concentrations; except for 10 μM MnTnOct-2PyP^{5+}. *Statistical difference ($p < 0.005$) from oxygen and glucose deprivation (OGD); † statistically equal ($p > 0.999$) to control.

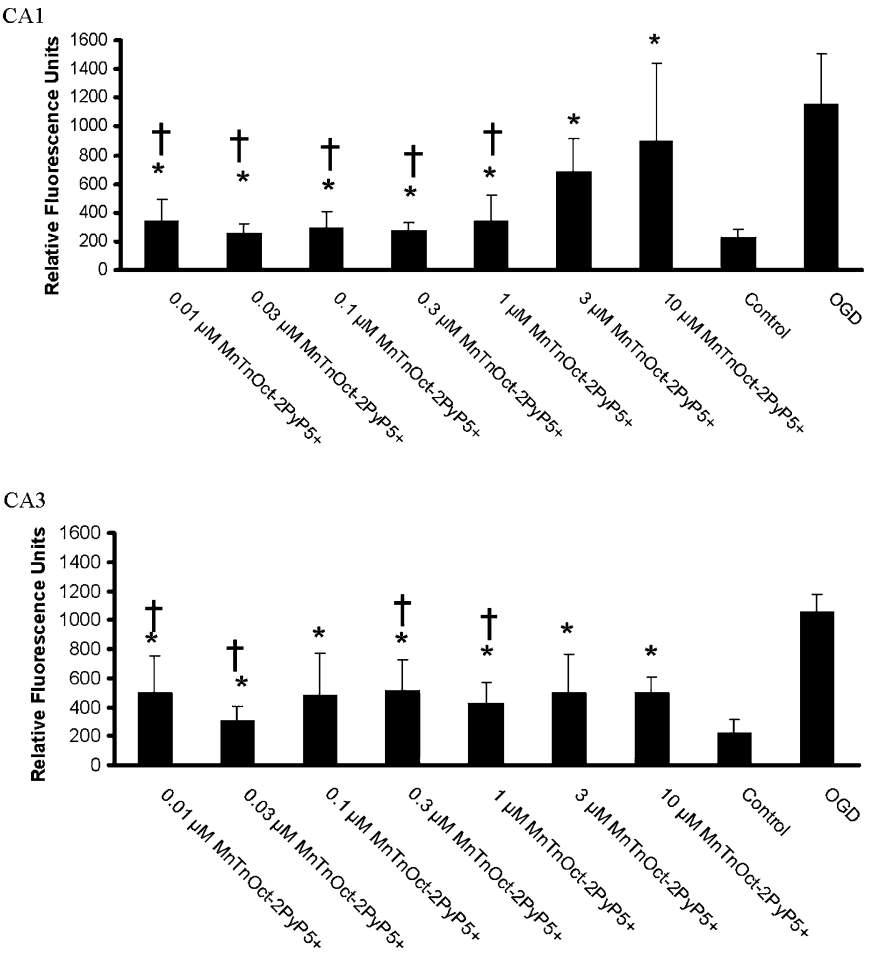

Figure 5. Cell death/Sytox staining of organotypic hippocampal slices (OHS): 30 min pre-treatment prior to exposure to oxygen and glucose deprivation with continued exposure during 45 min of oxygen and glucose deprivation—effects of submicromolar concentrations of MnTnOct-2-PyP^{5+}; 18–24 slices were examined for each condition. Relative fluorescence units ± SD are reported for each condition ($p < 0.05$). Areas CA1 (A) and CA3 (B) were evaluated. Regardless of region examined the data represents a statistical reduction in cell death with all concentrations of MnTnOct-2-PyP^{5+} as compared to OGD. All concentrations, except for 3 μM and 10 μM MnTnOct-2-PyP^{5+}, reduced neuronal cell death similar to control. There was no statistical difference among the concentrations studied except for 3 μM and 10 μM MnTnOct-2-PyP^{5+}. *Statistical difference ($p < 0.005$) from oxygen and glucose deprivation (OGD); †statistically equal ($p > 0.999$) to control.

full benefit of MnTnOct-2-PyP^{5+} was observed again at concentrations as low as 0.01 μM.

Discussion

Using our organotypic hippocampal slices model, we were able to clarify the efficacy of submicromolar concentrations of MnTnOct-2-PyP^{5+} under oxygen and glucose deprivation using fluorescent as opposed to spectrophotometric analysis. Both means of fluorescent imaging, propidium iodide and Sytox, provided similar data (Figures 4 and 5). Concentrations in the range of 0.01–3 μM of MnTnOct-2-PyP^{5+} exert remarkable neuronal protection in the presence of OGD which is up to 1000-fold higher than afforded by its hydrophilic analogues, MnTE-2-PyP^{5+} and MnTDE-2-ImP^{5+}.

Superoxide dismutases are first lines of defense, maintaining steady state levels of superoxide, and thus of all other reactive species formed downstream including peroxynitrite. MnSOD (SOD2) is one of the four major superoxide dismutases and is distributed in the mitochondrial matrix [33,34] and abundant in neural tissue. Under pathological conditions, endogenous SOD may not be able to offer sufficient protection. Thus, exogenous antioxidants may be beneficial. Several different classes have been studied, metalloporhyrins being among the most effective ones [7–24,34–36] . Our most potent compounds showed efficacy in nearly any model of oxidative stress tested, including central nervous system injuries [13–24]. MnTE-2-PyP^{5+} and MnTDE-2-ImP^{5+} (Figure 1) have demonstrated neuroprotection in a stroke model which is associated with a decrease in aconitase inactivation, 8-hydroxyguanine formation and cytokine expression [18,21].

Herein, for the first time we tested the octyl analogue, MnTnOct-2-PyP^{5+} (Figure 1) on the efficacy and toxicity. It is 1.4-fold more lipophilic

than hexyl porphyrin, MnTnHex-2-PyP^{5+} and ~6-fold more lipophilic than MnTE-2-PyP^{5+} and MnTDE-2-ImP^{5+} (as measured by thin layer chromatography R_f values, Table I); all four of them are of nearly identical SOD-like and $ONOO^-$-reducing activity (Table I) [7–12]. We have already shown that lipophilic MnTnHex-2-PyP^{5+} [9] is up to 120-fold more active *in vitro* and *in vivo* [13,22–24] in bacterial and mammalian models of oxidative stress (see Introduction). MnTnOct-2-PyP^{5+} was as effective as hexyl compound in protecting SOD-deficient *E. coli* [23]. Both hexyl and octyl porphyrins have partial micellar character and are thus toxic at higher doses, as observed here (Figures 4 and 5) and in *E. coli* study [23]. Yet the TD_{50} determined for mice to be 12.5 mg/kg (subcutaneously) is 250-times higher than its effective dose of 0.05 mg/kg, while the ratio is 15 with MnTE-2-PyP^{5+}, thus allowing a wider therapeutic window with MnTnHex-2-PyP^{5+} (Panni et al. 2008, unpublished). Similar is expected for octyl compound based on the effects observed in *E. coli* model [23].

The efficacy observed herein in protecting mixed neuronal/glial cells from oxygen and glucose deprivation with higher concentrations of MnTnOct-2-PyP^{5+} is comparable to or less than that of other two Mn porphyrins with fewer carbon atoms in the alkyl chains (Figures 2 and 3). The effects observed at concentration ≥ 3 μM were less than expected, as judged by propidium iodide (Figure 3) and LDH assay (Figure 2A and B) (where pre-treatment and treatment during deprivation was performed), and are *likely resulting from the interplay of efficacy and toxicity*. The remarkably protective effect of MnTnOct-2-PyP^{5+} in OHS against OGD at 0.01 μM concentration (Figures 4 and 5) suggests MnTnOct-2-PyP^{5+} might be a perspective antioxidant for therapeutic purposes. While MnTE-2-PyP^{5+} and MnTnOct-2-PyP^{5+} are equally potent antioxidants as measured by k_{cat} ($O_2^{\cdot-}$) and k_{red} ($ONOO^-$) (Table I), the higher efficacy in protecting cells against OGD is likely due to the increased bioavailability of octyl compound. Recently we were able to determine the partition coefficient of Mn alkylpyridylporphyrins between n-octanol and water, which is a common measure of drug lipophilicity. MnTE-2-PyP^{5+} has log $P_{ow} = -6.43$, while MnTnOct-2-PyP^{5+} has log $P_{ow} = -0.77$ (Table I) [37]. The 5.7 orders of magnitude increase in lipophilicty going from ethyl to octyl porphyrin parallels >3 orders of magnitude increase in efficacy found herein between ethyl and octyl porphyrin. The therapeutics that are widely used in clinics have log P_{ow} values varying from ~ −3 to ~ +5 [38,39]. Based on such values and on the data already obtained herein and elsewhere, MnTnOct-2-PyP^{5+} (log $P_{ow} = -0.77$) and MnTnHex-2-PyP^{5+} (log $P_{ow} = -2.29$) may be more promising drugs for clinical development than is MnTE-2-PyP^{5+}, particularly for central nervous system disorders.

In all four assays, MnTE-2-PyP^{5+} and MnTDE-2-ImP^{5+} were of comparable efficacy at concentrations ≥ 3 μM. Judged by LDH assay the former was a better performer, while based upon the propidium iodide assay the latter was performing better. All compounds show signs of toxicity at higher doses, which is consistent with toxicity found in the absence of OGD (Table II). Our findings are consistent with those obtained previously by Sheng et al. [18] on the effect of MnTDE-2-ImP^{5+} in mixed neuronal/glial cell cultures exposed to 2 h of oxygen and glucose deprivation. Given the very sensitive nature of neurons, the toxic effects, if any, are significantly lower than we expected. That is a motivating observation with respect to the future studies on the evaluation of the utility of MnTnOct-2-PyP^{5+} as a neuroprotective agent.

In conclusion, submicromolar concentrations of MnTnOct-2-PyP^{5+} in an *in vitro* rodent model of OGD are neuroprotective. The benefit of MnTnOct-2-PyP^{5+} in *in vivo* animal models needs to be further evaluated. The efficacy in therapeutic models of human injury remains to be defined.

Acknowledgements

LWF thanks the Multidisciplinary Neuroprotection Laboratories at Duke University Medical Center (NIH Grants T32 GM08600-09 and RO1 GM067139-03); IBH acknowledges the support by the National Institutes of Health (IR21-ESO/3682) and the National Institutes for Allergy and Infectious Diseases (U19AI067798) grants; William H. Coulter Translational Partners Grant Program. IS thanks NIH/NCI Duke Comprehensive Cancer Center Core Grant (5-P30-CA14236-29); the authors wish to thank Ms Candace Berryman for her editorial assistance.

***Declaration of interest*:** The authors report no conflicts of interest. The authors alone are responsible for the content and writing of the paper.

References

[1] Li QY, Pedersen C, Day BD, Patel M. Dependence of excitotoxic neurodegeneration on mitochondrial aconitase inactivation. J Neurochem 2001;78:746–755.

[2] Van Empel VPM, Bertrand AT, Van Oort RJ, Van der Nagel R, Engelen M, Van Rijen HV, Doevendans PA, Crijns HJ, Ackerman SL, Sluiter W, De Windt LJ. EUK-8, a superoxide dismutase and catalase mimetic, reduces cardiac oxidative stress and ameliorates pressure overload-induced heart failure in the harlequin mouse mutant. J Am Coll Cardiol 2006;48:824–832.

[3] Salvemini D, Wang Z-Q, Zweier JL, Samouilov A, Macarthur H, Misko TP, Curie MG, Cuzzocrea S, Sikorski JA, Riley DP.

A nonpeptidyl mimic of superoxide dismutase with therapeutic activity ion rats. Science 1999;286:304–306.
[4] Goldstein S, Samuni A, Hideg K, Merenyi G. Structure-activity relationship of cyclic nitroxides as SOD mimics and scavengers of nitrogen dioxide and carbonate radicals. J Phys Chem A 2006;110:3679–3685.
[5] James AM, Cocheme HM, Smith RAJ, Murphy MP. Interactions of mitochondria-targeted and untargeted ubiquinones with the mitochondrial respiratory chain and reactive oxygen species. J Biol Chem 2005;28:21295–21312.
[6] Smith RAJ, Porteous CM, Ganes AM, Murphy MP. Delivery of bioactive molecules to mitochondria. Proc Natl Acad Sci USA 2003;100:5407–5412.
[7] Batinić-Haberle I, Benov L, Spasojević I, Hambright P, Crumbliss AL, Fridovich I. The relationship between redox potentials, proton dissociation constants of pyrrolic nitrogens, and in vitro and in vivo superoxide dismutase activities of Manganese(III) and Iron(III) cationic and anionic porphyrins. Inorg Chem 1999;38:4011–4022.
[8] Reboucas JS, DeFreitas-Silva G, Idemori YM, Spasojevic I, Benov L, Batinic-Haberle I. The impact of electrostatics in redox modulation of oxidative stress by Mn porphyrins. Protection of SOD-deficient E. coli via alternative mechanism where Mn porphyrin acts as a Mn-carrier. Free Radic Biol Med 2008;45:201–210.
[9] Batinic-Haberle I, Spasojevic I, Stevens RD, Hambright P, Fridovich IJ. Manganese(III) *Meso* Tetrakis *Ortho N*-alkylpyridylporphyrins. Synthesis, characterization and catalysis of $O_2^{\cdot-}$ dismutation. J Chem Soc Dalton Trans 2002;2689–2696.
[10] Batinic-Haberle I, Spasojevic I, Stevens RD, Hambright P, Neta P, Okado-Matsumoto A, Fridovich I. New class of potent catalysts of $O_2^{\cdot-}$ dismutation. Mn (III) methoxyethylpyridyl- and methoxyethylimidazolylporphyrins. *Dalton Trans* 2004;1696–1702.
[11] Ferrer-Sueta G, Batinic-Haberle I, Spasojevic I, Fridovich I, Radi R. Peroxynitrite scavanging by manganese (III) meso-tetrakis-(N-methylpyridyl) porphyrins. Chem Res Toxicol 1999;12:442–449.
[12] Ferrer-Sueta G, Vitturi D, Batinić-Haberle I, Fridovich I, Goldstein S, Czapski G, Radi R. Reactions of manganese porphyrins with peroxynitrite and carbonate radical anion. J Biol Chem 2003;278:27432–27438.
[13] Gauter-Fleckenstein B, Fleckenstein K, Owzar K, Jian C, Batinic-Haberle I, Vujaskovic Z. Comparison of two Mn porphyrin-based mimics of superoxide-dismutase (SOD) in pulmonary radioprotection. Free Radic Biol Med 2007;44: 982–989.
[14] Vujaskovic Z, Batinic-Haberle I, Rabbani ZN, Feng Q-F, Kang SK, Spasojevic I, Samulski TV, Fridovich I, Dewhirst MW, Anscher MS. A small molecular weight catalytic metalloporphyrin antioxidant with superoxide dismutase (SOD) mimetic properties protects lungs from radiation-induced injury. Free Radic Biol Med 2002;33:857–863.
[15] Moeller BJ, Batinic-Haberle I, Spasojevic I, Rabbani ZN, Anscher MS, Vujaskovic Z, Dewhirst MW. Effects of a catalytic metalloporphyrin antioxidant on tumor radioresponsiveness. Int J Radiat Oncol Biol Phys 2005;63:545–552.
[16] Piganelli JD, Flores SC, Cruz C, Koepp J, Young R, Bradley B, Kachadourian R, Batinic-Haberle I, Haskins K. A metalloporphyrin superoxide dismutase mimetic (SOD mimetic) inhibits autoimune diabetes. Diabetes 2002;51: 347–355.
[17] Sompol P, Ittarat W, Tangpong J, Chen Y, Doubinskaia I, Batinic-Haberle I, Mohammad Abdul H, Butterfield A, St Clair DK. Alzheimer's disease: an insight into the mechanisms of oxidative stress-mediated mitochondrial injury. Neuroscience 2008;153:120–130.
[18] Sheng H, Enghild JJ, Patel M, Batinic-Haberle I, Calvi C, Day BJ, Pearlstein RD, Crapo JD, Warner DS. Effects of metalloporphyrin catalytic antioxidants in experimental brain ischemia. Free Radic Biol Med 2002;33:947–961.
[19] Sheng H, Batinic-Haberle I, Warner DS. Catalytic antioxidants as novel pharmacologic approaches to treatment of ischemic brain injury. Drug News Persp 2002;15:654–665.
[20] Leinenweber SB, Sheng H, Lynch JR, Batinic-Haberle I, Laskowitz DT, Crapo JD, Pearlstein RD, Warner DS. Effects of a manganese(III) porphyrin catalytic antioxidant in a murine model of closed head injury. Eur J Pharmacol 2006;531:126–132.
[21] Mackensen GB, Patel M, Sheng H, Calvi C, Batinic-Haberle I, Day BJ, Liang LP, Fridovich I, Crapo JD, Pearlstein RD, Warner DS. Neuroprotection from delayed post-ischemic administration of a metalloporphyrin catalytic antioxidant. J Neurosci 2001;21:4582–4592.
[22] Batinic-Haberle I, Ndengele MM, Cuzzocrea S, Reboucas JS, Masini E, Spasojevic I, Salvemini D. Lipophilicity is a critical parameter that dominates the efficacy of metalloporphyrins in blocking morphine tolerance through peroxynitrite-mediated pathways. Free Radic Biol Med 2008;46:212–219.
[23] Okado-Matsumoto A, Batinic-Haberle I, Fridovich I. Complementation of SOD-deficient Escheria Coli by manganese porphyrin mimics of superoxide dismutase activity. Free Radic Biol Med 2004;37:401–410.
[24] Saba H, Batinic-Haberle I, Munusamy S, Mitchell T, Lichti C, Megyesi J, Mac-Millan-Crow LA. Manganese porphyrin reduces renal injury and mitochondrial damage during ischemia/reperfusion. Free Radic Biol Med 2007;42:1571–1578.
[25] Wise-Faberowski L, Aono M, Pearlstein RD, Warner DS. Apoptosis is not enhanced in primary mixed neuronal/glial cultures protected by isoflurane against N-methyl-d-aspartate excitotoxicity. Anesth Analg 2004;99:1708–1714.
[26] Dugan LL, Gabrielsen JK, Yu SP, Lin TS, Choi DW. Buckminsterfullerenol free radical scavengers reduce excitotoxic and apoptotic cell death of cultured cortical neurons. Neurobiol Dis 1996;3:129–135.
[27] Wise-Faberowski L, Raizada MK, Sumners C. Oxygen and glucose deprivation-induced neuronal apoptosis is attenuated by halothane and isoflurane. Anesth Analg 2001;93:1281–1287.
[28] Stoppini L, Buch PA, Muller D. A simple method for organotypic cultures of nervous tissue. J Neurosci Methods 1991;37:173–182.
[29] Wise-Faberowski L, Zhang H, Ing R, Pearlstein RD, Warner DS. Isoflurane-induced neuronal degeneration: an evaluation in organotypic hippocampal slice cultures. Anesth Analg 2005;101:651–657.
[30] Batinic-Haberle I, Spasojevic I, Stevens RD, Bondurant B, Okado-Matsumoto A, Fridovich I, Vujaskovic Z, Dewhirst MW. New PEG-ylated Mn (III) porphyrins approaching catalytic activity of SOD enzyme. Dalton Trans 2006; 617–624.
[31] Moldrich RX, Beart PM, Pascoe CJ, Cheung NS. Low-affinity kainate receptor agonists induce insult-dependent apoptosis and necrosis in cultured murine cortical neurons. J Neurosci Res 2000;59:788–796.
[32] Cheung NS, Beart PM, Pascoe CJ, John CA, Bernard O. Human Bcl-2 protects against AMPA receptor-mediated apoptosis. J Neurochem 2000;74:1613–1620.
[33] Fridovich I. Superoxide anion radical ($O_2^{\cdot-}$), superoxide dismutase and related matters. J Biol Chem 1997;272: 25071–25076.
[34] Warner DS, Sheng H, Batinic-Haberle I. Oxidants, antioxidants and the ischemic brain. J Exp Biol 2004;207:3221–3231.

[35] Spasojevic I, Chen Y, Noel TJ, Fan P, Zhang L, Reboucas JS, St Clair DK, Batinic-Haberle I. Potent redox modulator of oxidative stress, MnTE-2-PyP^{5+}. Pharmacokinetics in mouse plasma, liver, kidney, spleen, lung, heart and brain. Free Radic Biol Med 2008;45:943–949.
[36] Spasojevic I, Yumin C, Noel T, Yu I, Pole MP, Zhang L, Zhao Y, St Clair DK, Batinic-Haberle I. Mn porphyrin-based SOD mimic, MnTE-2-PyP5+ targets mouse heart mitochondria. Free Radic Biol Med 2007;42:1193–1200.
[37] Kos I, Reboucas JS, Batinic-Haberler I. Lipohilicity of Mn(III) N-alkylpyridylporphyrins as measured by chromatographic means and partition between n-octanol and water; 2008, Free Radic Biol Med, Submitted.
[38] Hansch C, Leo A, Mekapati SB, Karup A. QSAR & ADMS. Bioorg Med Chem 2004;12:3391–3400.
[39] Proudfoot JR. The evolution of synthetic oral drug properties. Bioorg Med Chem Lett 2005;15:1087–1090.

This paper was first published online on iFirst on 4 March 2009.